Temperature Dependency of Photoelectronic Properties of Group III-V Arsenide Solar Cell

Md. Abdullah Al Humayun

Department of EEE, Eastern University, Bangladesh
humayun0403063@gmail.com

Masum Hossen

Department of EEE, Green University of Bangladesh, Bangladesh
masum.eee007@gmail.com

Md. Zamil Haider

Department of EEE, Eastern University, Bangladesh
mzhs.eee@gmail.com

Bedir Yousif

Department of Electrical Engineering, College of Engineering and Information Technology, Onaizah Colleges, Qassim, Saudi Arabia | Electrical Engineering Department, Faculty of Engineering, Kafrelsheikh University, Egypt
bedir.yousif@eng.kfs.edu.eg

Muhammad Tajammal Chughtai

Department of Electrical Engineering, College of Engineering, University of Hail, Saudi Arabia
mt.chughtai@uoh.edu.sa

Muhammad Islam

Department of Electrical Engineering, College of Engineering, Qassim University, Buraydah 51452, Saudi Arabia
muha.khan@qu.edu.sa (corresponding author)

Sheroz Khan

Department of Electrical Engineering, College of Engineering and Information Technology, Onaizah Colleges, Qassim, Saudi Arabia
cnar32.sheroz@gmail.com

ABSTRACT

This study explores the effect of temperature on different characteristics of Solar Cells (SC) composed of a structured III-V arsenide group. The temperature dependence of the SC characteristics was investigated numerically and by simulation. In both approaches, each characteristic was compared with a conventional Si SC. InAs showed superior stability and lower temperature sensitivity, as it has a negligible decrease of 0.098 eV in the energy bandgap, while the energy bandgaps of Si, AlAs, and GaAs are 0.129, 0.186, and 0.200 eV, respectively. Moreover, with a decay rate of 81.911 mV/°K, InAs exhibited the lowest temperature sensitivity in open-circuit voltage. InAs additionally demonstrated the least increase in degradation rate, while the SC power output is still a cause of concern. AlAs, Si, and GaAs had a total accumulative gradient change of 0.162, 0.136, and 0.034% in the degradation rate, respectively, while InAs showcased the highest stability by displaying a change of only 0.008%. A comparative analysis illustrated

that among these III-V arsenide compounds, InAs had a rock-bottom sensitivity to temperature changes and better temperature stability in both numerical and simulation approaches.

I. INTRODUCTION

Conventional energy sources are limited and are gradually diminishing day by day. In addition, the consumption of fossil fuels is producing CO_2 and other toxic gases that pollute the environment at an alarming rate. To overcome dependence on traditional energy sources, such as coal, gas, biomass, and others, it is necessary to satisfy our daily energy demands through alternative sources. Today, energy needs are constantly increasing in parallel with the raise in industrial development, the population augmentation, and lifestyle. Solar energy harvesting is an alternative source. The light energy coming from the Sun on Earth (120,000 TW of sunlight) is almost 20000 times more than the energy required to maintain daily activities on Earth [1-4]. SC is the "Eureka" for using this abundant amount of solar energy since it converts light into electrical energy. Moreover, it is a means of maneuvering energy from a natural fusion reactor in the sky, the Sun, and constitutes a possible solution to prevent climate change and environmental pollution. However, there are several challenges, such as high costs, low efficiency, and complex manufacturing processes, that slow down the growth of this technology [5]. Therefore, new materials are thoroughly studied to bypass these deficiencies. The use of new materials may advance the development and manufacturing of SCs and create an easy pathway to access clean, abundant, and affordable energy for all [6].

Silicon (Si) is the most widely employed material for SC fabrication. It has become convenient for the generation of electron-hole pairs of the depletion region in the crystal to move up and down to opposite polarities, creating a stronger electric field when exposed to light rather than vibrating in place and generating heat [7-8]. However, the process of developing or cultivating large crystals is very expensive due to the difficulty in growing them. In addition, it comes with material waste as a result of the need to slice it into thin films from its single-crystalline form of ingot, which are reshaped and converted into very thin slices called silicon wafers. The latter are called the hearts of an SC. SCs consisting of silicon are the first generation of solar cells, which are manufactured and used on a large scale and divided into monocrystalline and polycrystalline silicon SCs [9-10]. The absorption coefficient of Si decreases with the increasing wavelength of incident light photons. Therefore, researchers have introduced binary semiconductor compounds of GaAs, InAs, and AlAs as active layers for use in SCs to enhance cell efficiency, thus making solar energy more affordable. The theoretical limit for solar efficiency has been reported to will have achieved 40% by 2040 [11-12].

However, researchers are putting their efforts into increasing this efficiency figure so that this limitation will soon be overcome by tandem cells and thin-film SCs [13-15]. The highly intrinsic features of group III-V elements, such as direct energy bandgaps, high optical absorption coefficients, and good values for minority carrier lifetime and mobility, make

III-V arsenide compounds of GaAs, InAs, AlAs excellent candidate materials for the fabrication of high-efficiency SCs [14-15]. Many researchers have acknowledged that low-cost materials have the potential to be applied in SCs because they are suitable for absorbing energy from the solar spectrum [16-17]. The bandgap energy of the material is the most important characteristic that controls the properties of the SC, namely open circuit voltage, short-circuit current, and output power. Therefore, this study investigated the temperature dependence of these parameters for SCs using Group-III Arsenide and examined the performance of single-junction SCs. This study also considered an improved technique for generating solar energy from alarmingly high temperatures. The analysis which was conducted can be used to further study the temperature-dependent performance of thin-film multijunction SCs.

II. MATERIAL AND METHOD

A. Device Structure

Figure 1 shows a Quantum Dot SC (QDSC) grown with InAs QD layers [17-18] in 20 iterations. Each layer is isolated from the neighboring by a 15 nm GaAs spacer [19]. The QD layers are made from 2.5ML of InAs, covered with a 15 nm GaAs coating to sandwich the QD layers. In addition, the p-i-n structure of the QDSC was designed with a dielectric having a thickness of 200 nm of n-GaAs buffer layer, n-$Al_{0.33}Ga_{0.67}As$ of thickness 30 nm, 300 nm of n-GaAs base, emitter with 250 nm thick p-GaAs, 30 nm p-$Al_{0.75}Ga_{0.25}As$ window, and 250 nm thick p+-GaAs contact layer.
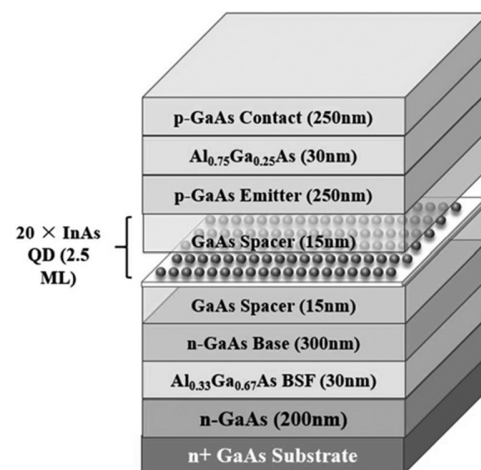

Fig. 1.   Schematic diagram of the QDSC structure.

B. Numerical Analysis

The major characteristics of QDSC were analyzed using Si, InAs, GaAs, and AlAs QD as the active layer material of the QDSC structure. The characteristics of the QDSC analyzed were open-circuit voltage, short-circuit current, output power, and temperature stability. The effect of temperature on the

energy bandgap of semiconductors has been explored in Varshni's model, given by [18]:

$$E_g(T) = E_g(0) - \frac{\gamma T^2}{(T+\beta)} \qquad (1)$$

where $E_g(T)$ is the semiconductor bandgap energy at a given temperature T, $E_g(0)$ is the bandgap value at 0°K, and γ and β are Varshni constants. The bandgap is one of the most important semiconductor parameters in solid-state physics. Variations in bandgap energy with temperature changes affect the overall performance of the solar cell, as it determines the absorption band of the cells.

By performing the derivation of the band gap $E_g(T)$ for temperature, the rate of change or the bandgap temperature reliance can be discussed with the help of the following calculations:

$$\frac{dE_g}{dT} = -\gamma \frac{T(T+2\beta)}{(T+\beta)^2} \qquad (2)$$

The negative sign in (2) indicates that the bandgap energy of the semiconductor decreases with increasing temperature values and vice-versa. To determine the magnitude of the rate of fluctuation of E_g volatility by taking the scales on both sides of (2) gives:

$$\left| \frac{dE_g}{dT} \right| = \gamma \frac{T(T+2\beta)}{(T+\beta)^2} \qquad (3)$$

The open circuit voltage, which is an important characteristic parameter of an SC device, can be determined according to:

$$V_{oc} = \frac{E_g(T)}{q} \qquad (4)$$

where q is the electric charge and $E_g(T)$ is the bandgap energy at temperature T of the active layer material of the SC structure. To analyze the temperature effect on the rate of change of open circuit voltage (V_{oc}), it is necessary to differentiate the V_{oc} equation to temperature:

$$\frac{dv_{oc}}{dT} = \frac{1}{q} \frac{dE_g}{dT} \qquad (5)$$

The open circuit voltage of the solar cell depends on the band gap energy of the active layer material in the solar cell and can be evaluated using:

$$I_{SC} = I_S e^{\left(\frac{q V_{oc}}{KT} - 1 \right)} \qquad (6)$$

where I_s is the saturation current of the binary material used in the active layer, q is the electric charge, K is Boltzmann's constant, and T is the absolute temperature in K. Both sides of (6) should be derived to explore the rate of short-circuit current degradation as a function of temperature, leading to:

$$\frac{dI_{SC}(T)}{dT} = \frac{qI_s}{KT^2} \left(\frac{TdV_{oc}(T)}{dT} - Voc \right) e^{\left(\frac{qv_{oc}}{KT} - 1 \right)} \qquad (7)$$

One of the parameters that affect the performance of the SC is the output power P_{out}, which can be obtained by:

$$P_{out}(T) = V_{oc}(T) * I_{SC}(T) \qquad (8)$$

where V_{oc} and I_{sc} are the open circuit voltage and short circuit current, respectively. To examine the change in the output power of the solar cell caused by temperature fluctuations, (8) is differentiated by the temperature to obtain:

$$\frac{dP_{out}(T)}{dT} = V_{oc}(T) \frac{dI_{SC}(T)}{dT} + I_{SC}(T) \frac{dV_{oc}(T)}{dT} \qquad (9)$$

C. Simulation Model

This section presents the simplified schematic diagram of the simulation model of the proposed QDSC using MATLAB Simulink. This study associated the achieved results of SC characteristics through the numerical approach with the characteristics obtained from simulation results to show the accuracy of the QDSC model. The SC characteristics, such as V_{oc}, I_{SC}, and P_{out}, have been measured at ambient conditions for four different QD materials as the active layer materials of the device structure. Figure 2 presents the QDSC models developed using Simulink.
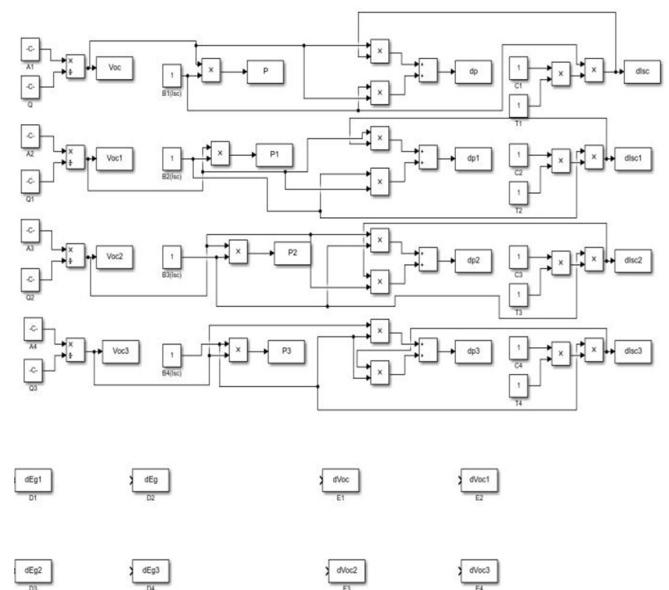

Fig. 2.   Simplified schematic diagram of the simulation model developed for the proposed QDSC structure using MATLAB Simulink.

III.   RESULTS AND DISCUSSION

The numerical analysis discloses the effects of temperature on the bandgap energy of the active layer material of SC, open circuit voltage, short circuit current, and the output power of SC. Table I depicts the values of some of the primary parameters necessary to analyze the performance characteristics of SC [21-23].

TABLE I.   BANDGAP ENERGY PARAMETERS FOR SI, GAAS, INAS, ALAS

Material	$E_g(0)$ [eV]	γ [eV/°K]	β [°K]
Si	1.17	4.73×10⁻⁴	636
GaAs	1.521	5.58×10⁻⁴	220
InAs	0.414	2.5×10⁻⁴	75
AlAs	2.239	6.0×10⁻⁴	408

Figure 3 illustrates the degradation of bandgap energy E_g for GaAs, AlAs, and InAs for the temperature over the range of

300-700°K along with the most widely used material Si to design SCs. The photovoltaic properties of the device are highly dependent on the E_g of the material used in the active layer of the device. In this figure, the dotted, solid, dash-dot, and dashed lines represent the respective E_g of Si, InAs, GaAs, and AlAs. The E_g of the materials utilized in this numerical analysis is gradually reducing nonlinearly with a uniform increase in temperature over the range of 300-700°K. The decrease in E_g occurs as the spacing between atoms increases, and this happens when the amplitude of atomic vibrations increases due to the rise in thermal energy. The resulting plot shows that Si experienced a decrease of 0.129eV in the bandgap energy, from 1.125eV to 0.997eV over the temperature range. AlAs decreased by 0.186 eV. Remarkably, GaAs had the highest downward trend in the energy bandgap of 0.200 eV, from 1.424 eV to 1.224 eV. However, InAs has experienced the lowest bandgap drop of 0.098 eV. The results obtained through numerical analysis and simulation show a good agreement.
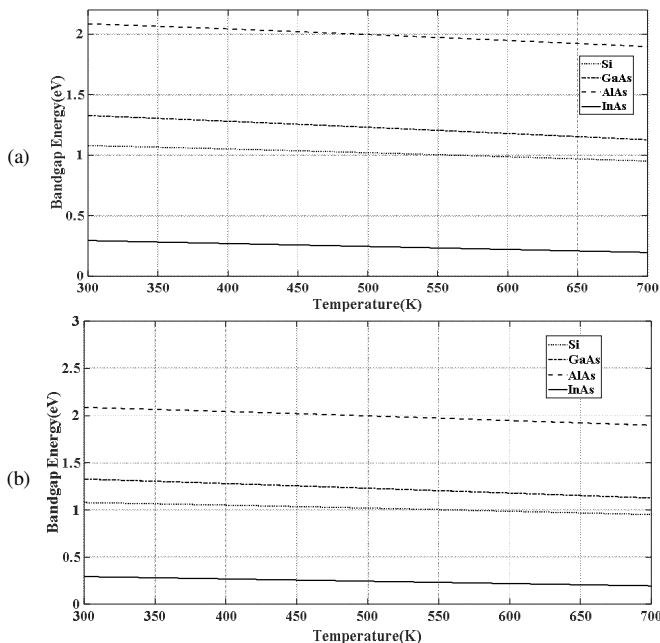

Fig. 3.   Degradation of bandgap energy of III-V arsenide material and Si with the increase in temperature: (a) Numerical analysis and (b) simulation results.

Figure 4 portrays the rate of change in E_g of Si, GaAs, AlAs, and InAs to temperatures in the range of 300-700°K. The rate of change of E_g of the active layer material of the SC decreases with an increase in temperature. InAs experiences a flat rate of change of 0.82%, while it has a rate of change from 24, 24.56, and 24.77 at 300, 500, and 700°K respectively. After undergoing extreme fluctuations of 18.75% and 7.37% against the temperate changes over the 300-500°K range, both AlAs and GaAs tend to have a relatively planar value throughout 500-700°K. However, compared to III-V arsenide materials, Si demonstrated the lowest stability against temperature. An overall volatility of 28% was observed, while the fluctuation in the first half was more than in the past. Si has a rate of change

of 25.59 meV/°K at 300°K and 32.63 meV/°K at 500°K. Using InAs in the SC active layer, the fluctuations in the rate of change of E_g were greatly reduced. The numerical and simulation results show a good agreement.
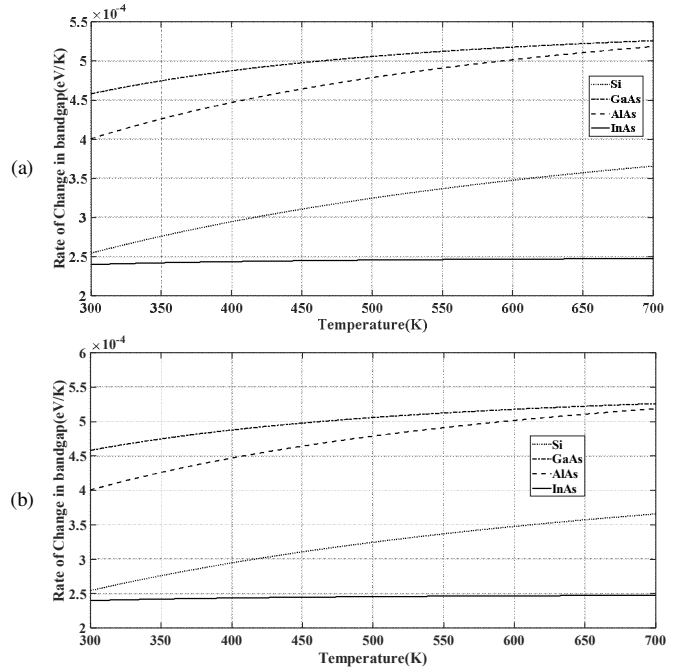

Fig. 4.   Rate of change in bandgap energy of III-V arsenide material and Si with the increase in temperature: (a) Numerical analysis and (b) simulation output.

Figure 5 exhibits the temperature reliances (V_{oc}) of the SC using Si, GaAs, AlAs, and InAs in the active layer for temperatures within the 300-700°K range. The corresponding changes in the V_{oc} of SC for Si, InAs, GaAs, and AlAs as active layers are represented by the dotted, solid, dash-dot, and dashed lines, respectively. The V_{oc} of SC undergoes a decrease as the temperature reaches higher values. The V_{oc} of the AlAs SC suddenly decreased from 2.09 to 1.91 V as the temperature increased from 300 to 700°K. However, it showed a gradual decrease after the temperature of 500°K, where V_{oc} is 2.01 V. The GaAs SC had a total decrease of 0.19 V in V_{oc}, while for Si this value was 0.14 V. The InAs SC had a minimum drop in V_{oc} and experienced a total drop of 0.10 V with an increase in temperature from 300 to 700°K. The results obtained through numerical analysis and simulation reveal a good agreement.

Figure 6 depicts the rate of change of V_{oc} using Si, GaAs, AlAs, and InAs in the active layer of the SC structure for temperatures in the 300-700°K range. The rate of change in Voc decreased significantly by employing InAs, while it had an overall increase of 0.446 μV/°K in the degradation rate. However, both AlAs and GaAs had a considerable increase in the degradation rate of 0.595 μV/°K and 0.776 μV/°K, accordingly, for the total temperature variation. In contrast to the application of III-V Arsenide as the active layer material, conventional Si possesses poor stability against temperature variations. The rate of change in V_{oc} of SC is greatly increased for Si after 500°K. The slope of the curve experienced an

exponential of 480.81 µV/°K in the rate of change of V_{oc}, where it decreased by a rate of 1036.36 µV/°K in V_{oc} at 700°K and 555.55 µV/°K mV increase at 500°K. Again, the outcomes obtained through numerical analysis and simulation disclose good agreement.
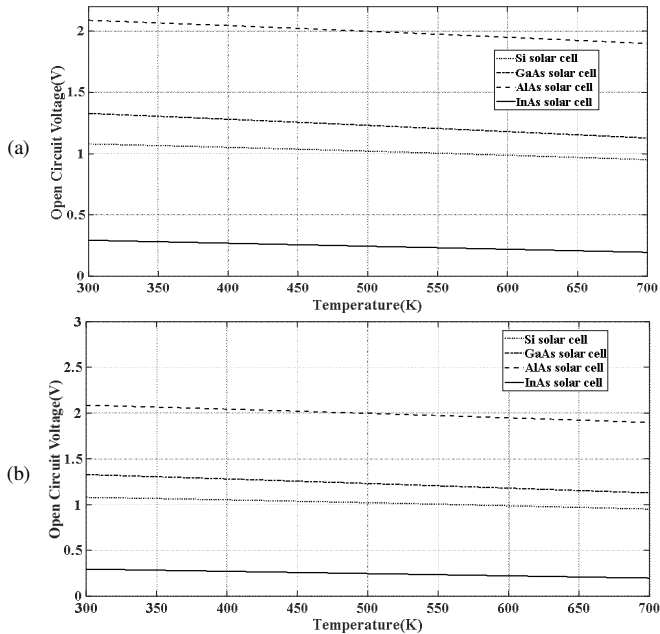

Fig. 5.   Dependency of open circuit voltage (V_{oc}) of SC on temperature fluctuation: (a) Numerical analysis and (b) simulation output.
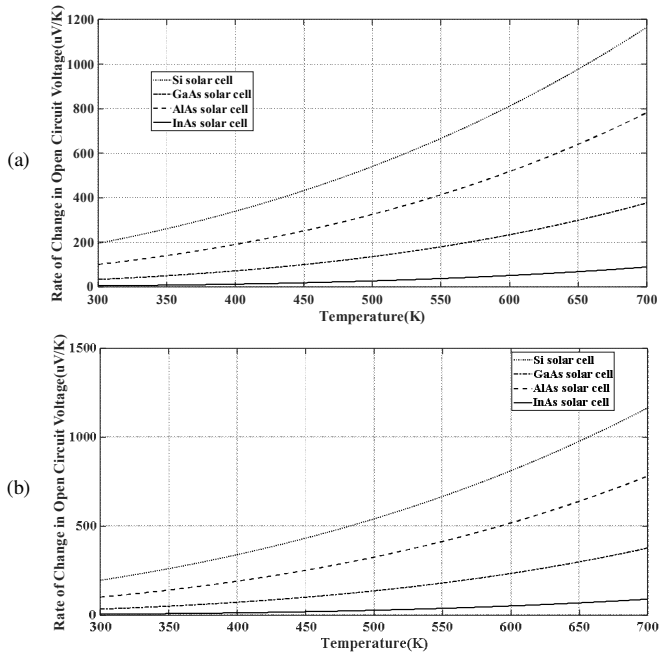

Fig. 6.   Rate of change of open circuit voltage against temperature fluctuations: (a) Numerical analysis and (b) simulation output.

Figure 7 illustrates the dependency of I_{sc} of SCs with Si, GaAs, AlAs, and InAs in the active layer of their structure for

temperatures within 300°K-700°K. The dotted, solid, dash-dot, and dashed lines represent the SCs having Si, InAs, GaAs, and AlAs in their active layer. The AlAs SC decreased by 0.40% after 500°K. Si and GaAs SCs presented quite similar sensitivity to temperature and had a gradual decrease in short circuit currents of 0.21% and 0.27%, correspondingly. The InAs SC demonstrated better stability, as it experienced only a decrease of 0.07% in the same temperature range. Again, the results obtained through numerical analysis and simulation show good agreement.
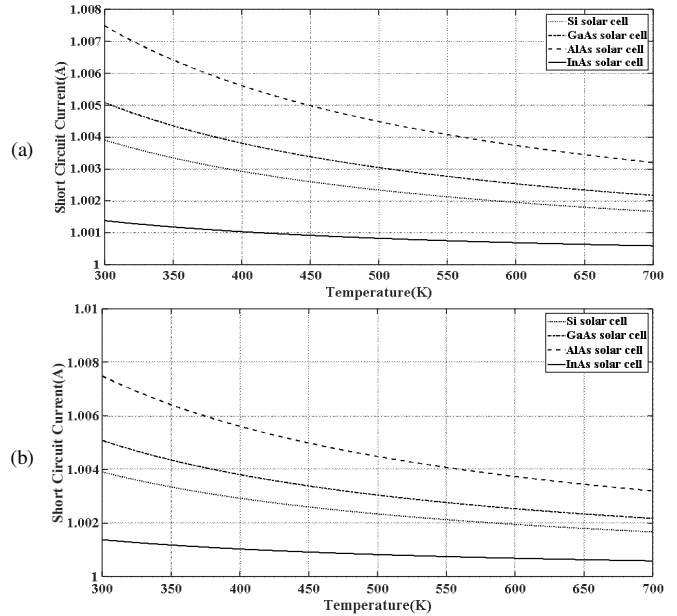

Fig. 7.   Dependency of short circuit current of SC on the temperature fluctuations: (a) Numerical analysis and (b) simulation output.
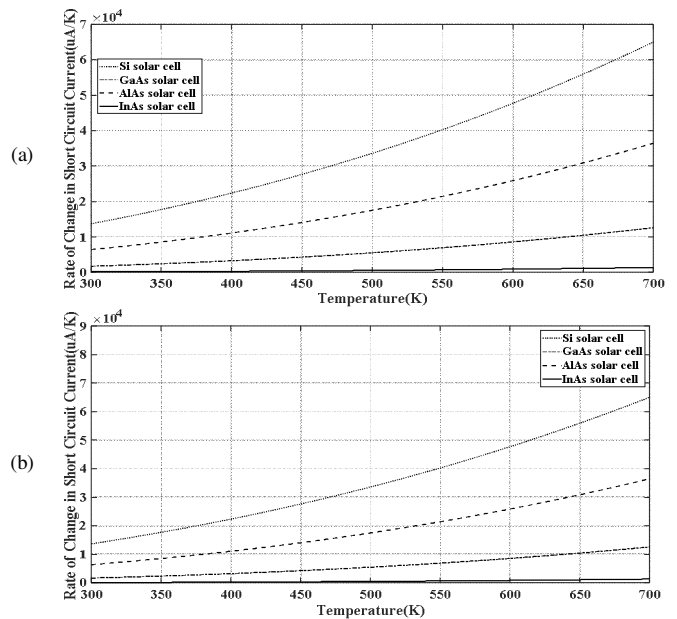

Fig. 8.   Rate of change in short circuit current of SC due to temperature fluctuations: (a) Numerical analysis and (b) simulation output.

Figure 8 verifies the nominal decrease in the rate of change of I_{sc} of SCs as the temperature increases. Conventional Si SC showed the worst stability at high temperatures and had the most upward fluctuations of 6.01 µAmp/°K in the rate of change of I_{sc} as temperature increased from 300 to 700°K. The instability gradually increased for AlAs and GaAs SCs, although GaAs SC displayed a lower drift rate compared to the AlAs SC. However, InAs brings out as a promising compound for use in SCs by exhibiting an overall lower increase of 0.11 µAmp/°K in the I_{sc} value compared to other widely used AlAs, GaAs, and Si. Again, the numerical and simulation results show good agreement.

Output power P_{out} is generally considered to be one of the most reliable variables for measuring how well a device is performing for practical applications. Figure 9 presents the effect of temperature changes on the P_{out} of SC. In this plot, dotted, solid, dash-dot, and dashed lines illustrate the output power for temperature for SCs using Si, InAs, GaAs, and AlAs in the active layer of their structure. The general trend of P_{out} is downward with increasing temperature. The Si SC had a decrease of approximately 12%, as it has an output power of 1.09 and 0.96 nW at 300 and 700°K, respectively. InAs displayed a total output power drop of 0.10 nW, while GaAs SC had the highest loss of 0.19495 nW on P_{out} for the respective temperature change. Again, the results obtained through numerical analysis and simulation show good agreement.
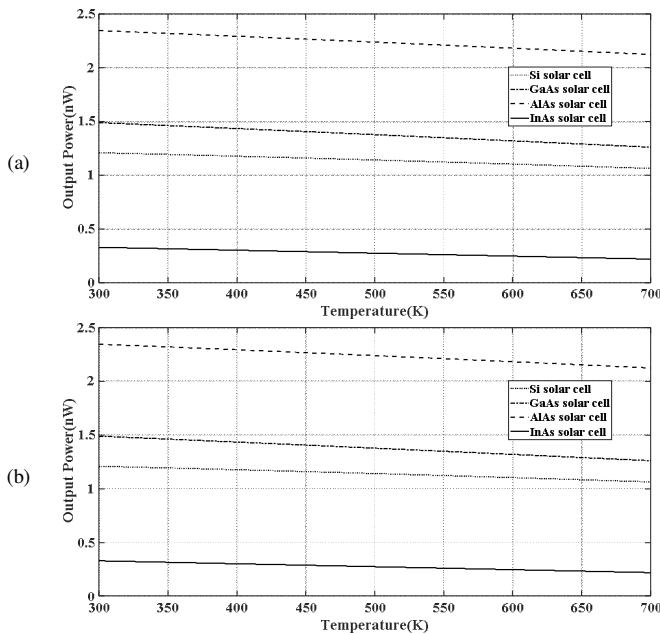

Fig. 9.   Change in output power of SC against temperature fluctuations: (a) Numerical analysis and (b) simulation output.

Figure 10 shows the amount of variation in P_{out} of SCs for temperature fluctuation per unit. Si and AlAs SCs showed a significant increase in the rate of change in P_{out}, but the AlAs SC exhibited significant sensitivity after 500°K. The AlAs SC had a lower P_{out} rate of change value than Si at 300°K (0.16 nW/°K) and ended with a value of 0.79 nW/°K at 700°K. The rate gradually increased for GaAs and ended with 0.17 nW/°K at 700°K. However, the analysis confirmed that the rate of change in the resulting P_{out} degradation was significantly reduced for the SC having InAs in its active layer structure, remaining nearly stable throughout the temperature fluctuation. Figure 10 clearly indicates that the GaAs SC had an acceptable reduction rate in P_{out}. However, conventional Si and AlAs had an intense upward rate of power degradation. Again, the numerical and simulation results show good agreement.
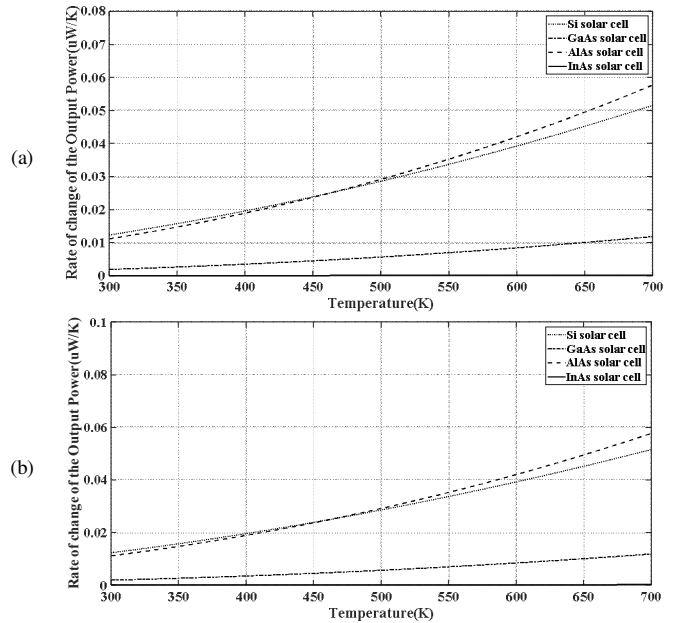

Figure 10: Rate of change of the output power of SC due to temperature fluctuations: (a) Numerical analysis and (b) simulation output.

IV.   CONCLUSION

This study investigated the temperature dependence of the open circuit voltage (V_{oc}) and short circuit current (I_{sc}) of SCs within a temperature range of 300 to 700°K to determine their output power (P_{out}). The numerical results acquirerd were compared with an SC using Si as active layer material. To examine these characteristics, the temperature dependence of the bandgap energy of III-V Arsenide material and Si was analyzed with a temperature range of 300 to 700°K, since it governs the SC characteristics. Much of the solar energy is not taken into account, as the SC cannot cover the entire solar band (specifically, ultraviolet, infrared, and low or diffused light) into electrical energy. Moreover, the stability of the photovoltaic properties is also very crucial for SCs. Materials with high stability and low bandgap can be a concern for tandem cells, which split light into different wavelength bands, produce a different color of light, and direct the beams to different cells tuned to those bands. GaAs demonstrated good integrity at low temperatures and had a satisfactory bandgap energy for SC designs. Therefore, GaAs can be considered as a potentially promising candidate material to be applied in SC design. SCs have the highest efficiency within an energy bandgap around 1.35-1.5 eV [24].

REFERENCES

[1] "The Balance of Power in the Earth-Sun System," National Aeronautics and Space Administration, 2005. [Online]. Available: https://www.nasa.gov/wp-content/uploads/2015/03/135642main_balance_trifold21.pdf.

[2] Y. Liang *et al.*, "Co₃O₄ nanocrystals on graphene as a synergistic catalyst for oxygen reduction reaction," *Nature Materials*, vol. 10, no. 10, pp. 780–786, Oct. 2011, https://doi.org/10.1038/nmat3087.

[3] "Solar Energy Source: Pros and Cons," *Canadian Institute For Knowledge Development*, Nov. 25, 2019. https://cikd.ca/2019/11/25/solar-energy-source-pros-and-cons/.

[4] N. S. Lewis and D. G. Nocera, "Powering the planet: Chemical challenges in solar energy utilization," *Proceedings of the National Academy of Sciences*, vol. 103, no. 43, pp. 15729–15735, Oct. 2006, https://doi.org/10.1073/pnas.0603395103.

[5] P. Balling *et al.*, "Improving the efficiency of solar cells by upconverting sunlight using field enhancement from optimized nano structures," *Optical Materials*, vol. 83, pp. 279–289, Sep. 2018, https://doi.org/10.1016/j.optmat.2018.06.038.

[6] K. Kumari, T. Chakrabarti, A. Jana, D. Bhattachartjee, B. Gupta, and S. K. Sarkar, "Comparative Study on Perovskite Solar Cells based on Titanium, Nickel and Cadmium doped BiFeOₛ active material," *Optical Materials*, vol. 84, pp. 681–688, Oct. 2018, https://doi.org/10.1016/j.optmat.2018.07.071.

[7] Q. H. Fan *et al.*, "High efficiency silicon–germanium thin film solar cells using graded absorber layer," *Solar Energy Materials and Solar Cells*, vol. 94, no. 7, pp. 1300–1302, Jul. 2010, https://doi.org/10.1016/j.solmat.2010.03.006.

[8] S. Kaci *et al.*, "Impact of porous SiC-doped PVA based LDS layer on electrical parameters of Si solar cells," *Optical Materials*, vol. 80, pp. 225–232, Jun. 2018, https://doi.org/10.1016/j.optmat.2018.05.006.

[9] C. Ji *et al.*, "Recent Applications of Antireflection Coatings in Solar Cells," *Photonics*, vol. 9, no. 12, Dec. 2022, Art. no. 906, https://doi.org/10.3390/photonics9120906.

[10] M. S. Almomani *et al.*, "Performance Improvement of Graded Bandgap Solar Cell via Optimization of Energy Levels Alignment in Si Quantum Dot, TiO₂ Nanoparticles, and Porous Si," *Photonics*, vol. 9, no. 11, 2022, https://doi.org/10.3390/photonics9110843.

[11] A. M. Mouafki, F. Bouaïcha, A. Hedibi, and A. Gueddim, "Porous Silicon Antireflective Coatings for Silicon Solar Cells," *Engineering, Technology & Applied Science Research*, vol. 12, no. 2, pp. 8354–8358, Apr. 2022, https://doi.org/10.48084/etasr.4803.

[12] S. V. Boriskina and G. Chen, "Exceeding the solar cell Shockley–Queisser limit via thermal up-conversion of low-energy photons," *Optics Communications*, vol. 314, pp. 71–78, Mar. 2014, https://doi.org/10.1016/j.optcom.2013.10.042.

[13] S. M. Ho, "Fabrication of Cu4SnS4 Thin Films: A Review," *Engineering, Technology & Applied Science Research*, vol. 10, no. 5, pp. 6161–6164, Oct. 2020, https://doi.org/10.48084/etasr.3663.

[14] M. Sojoudi, R. Madatov, T. Sojoudi, and P. Farhadi, "Achieving Steady and Stable Energy from AlGaAsGaAs Solar Cells," *Engineering, Technology & Applied Science Research*, vol. 1, no. 6, pp. 151–154, Dec. 2011, https://doi.org/10.48084/etasr.93.

[15] S. Guterman *et al.*, "Optimized flexible cover films for improved conversion efficiency in thin film flexible solar cells," *Optical Materials*, vol. 79, pp. 243–246, May 2018, https://doi.org/10.1016/j.optmat.2018.03.034.

[16] S. K. Tripathy and A. Pattanaik, "Optical and electronic properties of some semiconductors from energy gaps," *Optical Materials*, vol. 53, pp. 123–133, Mar. 2016, https://doi.org/10.1016/j.optmat.2016.01.012.

[17] E. V. Kunitsyna *et al.*, "Narrow gap III–V materials for infrared photodiodes and thermophotovoltaic cells," *Optical Materials*, vol. 32, no. 12, pp. 1573–1577, Oct. 2010, https://doi.org/10.1016/j.optmat.2010.06.010.

[18] S. Takatori *et al.*, "Investigation of the terahertz emission characteristics of MBE-grown GaAs-based nanostructures," *Optical Materials*, vol. 32, no. 7, pp. 776–779, May 2010, https://doi.org/10.1016/j.optmat.2010.02.014.

[19] P. M. Lam *et al.*, "Effect of rapid thermal annealing on InAs/GaAs quantum dot solar cells," *IET Optoelectronics*, vol. 9, no. 2, pp. 65–68, 2015, https://doi.org/10.1049/iet-opt.2014.0079.

[20] A. Mahfoud, F. Mohamed, S. Mekhilef, and F. Djahli, "Effect of Temperature on the GaInP/GaAs Tandem Solar Cell Performances," *International Journal Of Renewable Energy Research*, vol. 5, no. 2, pp. 629–634, Jun. 2015.

[21] J. Singh, *Physics of Semiconductors and Their Heterostructures*. New York, NY, USA: McGraw-Hill College, 1992.

[22] M. V. Fischetti and S. E. Laux, "Monte Carlo simulation of transport in technologically significant semiconductors of the diamond and zinc-blende structures. II. Submicrometer MOSFET's," *IEEE Transactions on Electron Devices*, vol. 38, no. 3, pp. 650–660, Mar. 1991, https://doi.org/10.1109/16.75177.

[23] V. A. Wilkinson and A. R. Adams, "The effect of temperature and pressure on InGaAs band structure," *EMIS Data Reviews Series*, vol. 8, 1993.

[24] G. Saint-Girons, A. Mereuta, G. Patriarche, J. M. Gérard, and I. Sagnes, "Influence of the thermal treatment on the optical and structural properties of 1.3 µm emitting LP-MOVPE grown InAs/GaAs quantum dots," *Optical Materials*, vol. 17, no. 1, pp. 263–266, Jun. 2001, https://doi.org/10.1016/S0925-3467(01)00089-1.